Avicenna Journal of Phytomedicine (AJP)

Original Research Article

Nano-eupatilin improves solubility and ameliorates dexamethasone-induced hyperlipidemia in male rats

Zeinab Yazdiniapour[1], Leila Safaeian[2,*], Erfaneh Ghassami[3], Samira Ghasemi[2]

[1]*Department of Pharmacognosy, School of Pharmacy and Pharmaceutical Sciences, Isfahan University of Medical Sciences, Isfahan, Iran*
[2]*Department of Pharmacology and Toxicology, Pharmaceutical Sciences Research Center, School of Pharmacy and Pharmaceutical Sciences, Isfahan University of Medical Sciences, Isfahan, Iran*
[3]*Department of Pharmaceutics, Novel Drug Delivery Systems Research Center, School of Pharmacy and Pharmaceutical Sciences, Isfahan University of Medical Sciences, Isfahan, Iran*

Article history:
Received: Jul 29, 2025
Received in revised form: Jul 12, 2026
Accepted: Jul 28, 2026
Epub ahead of print

**** Corresponding Author:***
leila_safaeian@pharm.mui.ac.ir

Keywords:
Chitosan
Eupatilin
Hyperlipidemias
Lipid peroxidation
Nanoparticles
Rats

Abstract

Objective: Eupatilin (EUP), as a natural flavone with various pharmacological properties, has a very low solubility in water. Nanoparticles have been widely used to increase the dissolution rate of drugs. This study aimed to assess the effect of nano-formulation of EUP in the form of EUP-loaded chitosan nanoparticles (EUP-NPs) on its solubility and to investigate its antihyperlipidemic potential in a model of hyperlipidemia induced by dexamethasone (DEX).

Materials and Methods: EUP-NPs were prepared using an ionotropic gelation procedure and their physicochemical properties were characterized. For induction of hyperlipidemia, DEX (10 mg/kg/day for 7 days) was injected subcutaneously in Wistar rats. Animals were randomized into seven groups, including: normal control, hyperlipidemic control, and hyperlipidemic rats which received EUP or EUP-NPs (50 and 100 mg/kg) or atorvastatin (40 mg/kg) as the reference group.

Results: EUP-NPs were entrapped effectively with a desirable particle size, polydispersity index (PDI) value, and controlled drug release. Saturated solubility test showed that the water solubility of EUP-NPs was increased about ten times compared to the free EUP. DEX led to a significant increase in serum lipid profile markers, atherogenic indices, lipid peroxidation, and liver enzymes activities. EUP-NPs (100 mg/kg) reduced the serum level of total cholesterol (20.55%, $p<0.01$), triglycerides (47.02%, $p<0.01$), low-density lipoproteins (28.69%, $p<0.05$), atherogenic indices (66.67%, $p<0.001$), malondialdehyde ($p<0.01$) and liver enzymes ($p<0.05$), and improved liver histopathologic abnormalities as compared to DEX hyperlipidemic group more effectively than free EUP.

Conclusion: This study revealed the higher water solubility for EUP-NPs, and more effective anti-hyperlipidemic and antioxidant activities in DEX-induced hyperlipidemia compared to free EUP.

Please cite this paper as:
Yazdiniapour Z, Safaeian L, Ghassami E, Ghasemi S. Nano-eupatilin improves solubility and ameliorates dexamethasone-induced hyperlipidemia in male rats. Avicenna J Phytomed, 2026

Introduction

Hyperlipidemia is defined as the elevation in the plasma concentration of lipids, including total cholesterol, triglyceride, and lipoprotein particles (Nasrullah et al. 2023). Global studies have shown that about 37% of male and 40% of female adults worldwide have hypercholesterolemia. Hyperlipidemia is one of the main risk factors for various cardiovascular diseases, such as atherosclerosis. About one-third of ischemic heart disease and 4.5% of all deaths are due to elevated cholesterol levels (WHO 2012). Hyperlipidemia is also associated with other diseases such as non-alcoholic fatty liver disease (Tomizawa et al. 2014). Numerous studies have revealed the important role of oxidative stress in the progression of atherogenic dyslipidemia and atherosclerosis (Vekic et al. 2023).

Oxidative stress, as a disequilibrium between oxidant factors and anti-oxidative defense, may lead to the oxidation of lipids and formation of oxidized low-density lipoproteins (LDL), which possess proinflammatory, thrombotic and atherogenic effects (Poznyak et al. 2021). Many herbal medicines and bioactive compounds have been shown to have beneficial antioxidant, antihyperlipidemic, and synergistic therapeutic activities in the management of dyslipidemia (Suganya et al. 2016).

Eupatilin (5,7-dihydroxy-3′, 4′, 6-trimethoxyflavone; EUP) is a plant flavone with potent antioxidant activity (Wang et al. 2025) (Figure 1). Flavones are a large group of flavonoids with nutritional value whose main nucleus is 2-phenyl-1-benzopyran-4-one (Jiang et al. 2016).

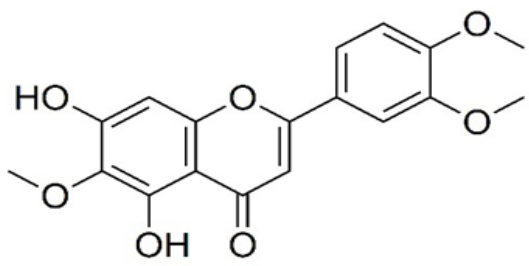

Figure 1. Chemical structure of eupatilin.

EUP is found in many plants of the Asteraceae family, including *Artemisia*, *Centaurea*, and *Tanacetum* species. This compound is also found in the Lamiaceae family and the *Salvia* genus (Nageen et al. 2020). EUP has a variety of pharmacological effects including anti-cancer, anti-inflammatory, anticoagulant, antiplatelet, and neuro-protective effects (Zhong et al. 2016; Min et al. 2009; Qiao et al. 2018; Ryu et al. 2013). Studies have described the antihyperlipidemic properties of some flavones such as apigenin and luteolin that are structurally very similar to the EUP (Xu et al. 2021; Sun et al. 2021). There are some reports of the antioxidant and anti-lipid-peroxidative activities for EUP (Rosa et al. 2020; Lee et al. 2020). In an *in vitro* assay, EUP was able to significantly protect cholesterol and fatty acids from oxidative damage and to modulate lipid profile (Rosa et al. 2020). In recent studies, EUP has shown lipid-lowering effects through several important mechanisms including the inhibition of 3-hydroxy-3-methylglutaryl (HMG)-coenzyme A (CoA) reductase as the rate-limiting enzyme of the mevalonate pathway which is an essential stage in the biosynthesis of cholesterol (Kim et al. 2023), the activation of peroxisome proliferator-activated receptor alpha (PPARα) as a major regulator of hepatic lipid metabolism (Choi et al. 2015), and the reduction of expression of PPARγ as a crucial regulator of adipogenesis (Kim et al. 2018). EUP also has anti-inflammatory activities by decreasing tumor necrosis factor (TNF)-α and interleukin (IL)-1β levels (Lee et al. 2020). Clinical evidence has revealed the relation between inflammation and hyperlipidemia in the development of atherosclerosis and arterial damage (Rodriguez-Garcia and Alcaide 2021). Moreover, hyperlipidemia is an important risk factor for thrombosis (Kawasaki et al. 1997). Investigations have shown that EUP markedly prevents thrombosis by diminishing the arachidonic acid-induced platelet aggregation and the

generation of serotonin and thromboxane A2 (Ryu et al. 2013).

Nevertheless, pharmacokinetic studies have shown that after oral administration, the bioavailability of EUP and its metabolite was 3.86%, of which 68.5% was not absorbed through the digestive tract (Jang et al. 2003; Geng et al. 2018). The solubility of EUP in water is very low and equal to 0.0402 mg/L (TMIC 2025). Appropriate drug carriers can solve many problems in drug delivery, such as low solubility, low bioavailability, side effects, low stability, etc. (Hu et al. 2004). Chitosan nanoparticles (NPs) are suitable carriers for drugs that can improve drug dissolution and stability, increase drug efficacy, and reduce toxicity (Wang et al. 2011).

In this study, we attempted to assess the effect of nano-formulation of EUP in the form of EUP-loaded chitosan nanoparticles (EUP-NPs) on its solubility and to evaluate its possible antihyperlipidemic and antioxidant properties in a model of hyperlipidemia induced by dexamethasone (DEX) in rats.

Materials and Methods

Chemicals and reagents

DEX (Darou Pakhsh Pharmaceutical Co., Iran), atorvastatin (ATOR) (Abidi Pharmaceutical Laboratories Co., Iran), chitosan (Sigma-Aldrich Co., Spain), and all other chemicals were acquired from Merck, Germany. The biochemical assay kits were obtained from Pars Azmoon Co. (Iran), and the malondialdehyde (MDA) assay kit from Hakiman Pajooh Research Co. (Iran).

Isolation and identification of EUP

In our previous study, EUP was isolated from all parts of *Artemisia kermanensis* Podl., which was collected from Taftan Mountain (Sistan and Baluchestan province of Iran) and maintained as a voucher specimen (No. 4001) at the Herbarium of the Department of Pharmacognosy, Isfahan University of Medical Sciences (Soleimanifard et al. 2023). Briefly, after preparation of the dichloromethane/acetone extract, fractionation was done through Medium-Pressure Liquid Chromatography (MPLC) using normal silica gel (particle size 15-40 µm) and a solvent system of hexane/ethyl acetate as the mobile phase. The obtained fractions were analyzed by Thin Layer Chromatography (TLC), and the flavonoid-containing fractions were subjected to the crystallization technique for separation of EUP. The final purification and identification of the structure of crystals as 5,7-dihydroxy-3',4',6-trimethoxyflavone was performed by Nuclear Magnetic Resonance (NMR), hydrogen (H)-NMR, UV (Ultraviolet), IR (Infrared), and mass spectroscopy.

Preparation of EUP-loaded nanoparticles (EUP-NPs)

EUP-NPs were prepared by an ionotropic gelation procedure (Kunjachan et al. 2010). For this, 0.4 g of chitosan was dissolved in 40 mL of aqueous acetic acid (1% v/v) containing mannitol (0.5% w/v) as a cryoprotectant and Tween 80 (0.2% w/v) as an emulsifier. Then the desired amount of EUP was dissolved in dichloromethane and methanol (1:1), and was gently dripped into the chitosan solution while continuously mixed under magnetic stirring. After that, tripolyphosphate (TPP) solution (0.5% w/v) was added drop-wise to establish cross-links. After evaporating the organic solvents, the final solution was centrifuged and the precipitated NPs were freeze dried.

Particle size and zeta potential measurement

The Zetasizer (Zetasizer 3600, Malvern Instrument Ltd., UK) was applied to evaluate the particle size, zeta potential, and polydispersity index (PDI) through the dynamic light scattering method. The sample was prepared by dispersing 10 mg of lyophilized powder of EUP-NPs in phosphate buffer saline (PBS) containing dimethyl sulfoxide (DMSO) (0.5%) at a

ratio of 1 to 10 through vortexing for 5 min. All the measures were performed in triplicate.

Saturated solubility test

Saturated solubility of the samples was assessed by taking the excess amounts of EUP-NPs or free EUP in deionized water. Each solution was shaken for 48 hr at 50 rpm. Then the supernatant was separated and diluted with PBS containing 0.5% DMSO (1:20) and analyzed spectrophotometrically at 233 nm.

Entrapment efficiency

For evaluation of drug entrapment efficiency, the amount of EUP that was loaded in the chitosan NPs was indirectly determined by measuring the drug content in the supernatant. The samples were prepared by dispersing the lyophilized EUP-NPs or blank (lyophilized NPs without EUP) in PBS containing DMSO and then centrifuging at 10,000 rpm for 15 min at 25 °C. After dilution of the supernatant (1:100), the absorbance of solutions was read at 233 nm and the entrapment efficiency was calculated based on the difference between the total and free EUP concentrations (Varshosaz et al. 2019).

In vitro drug-release evaluation

Drug release evaluation was performed using the dialysis technique in PBS medium containing DMSO (0.5%) at pH 7.4. The samples, including EUP-NPs, free EUP, and NPs without EUP (blank) were placed inside a dialysis bag (cut-off 10,000 Da) flooded with release medium. Drug release was assessed at 37°C for 2 hr, and 1 mL of the samples was taken at each specific time interval (15, 30, 45, 60, 90, and 120 min) and replaced with a fresh medium. After centrifugation, the absorbance of the samples was recorded by a UV spectrophotometer at 233 nm, and the studies were repeated three times.

Fourier transform infrared (FTIR) spectroscopy

The chemical composition of EUP-NPs was studied by FTIR spectroscopy. The spectra of samples including EUP-NPs and free EUP were obtained using an FTIR spectrometer (JASCO model 6300FV, Tokyo, Japan). The pellet samples were provided using potassium bromide during hydraulic press at a pressure of 10 tons force for 30 sec and scanned at a range of 4000-400 cm^{-1} with 4 cm^{-1} resolution.

Animals and treatment

Glucocorticoid-induced hyperlipidemia model was used to evaluate the blood lipid-lowering ability of the prepared EUP-NPs by subcutaneous (s.c.) administration of 10 mg/kg DEX for 7 days (Safaeian et al. 2018). Forty-two male Wistar rats (8-10 weeks old, 200-220 g) grown in the animal house of the School of Pharmacy and Pharmaceutical Sciences (Isfahan, Iran) were used in this study. Rats were housed at standard laboratory conditions of 20-25 ºC with standard diet and water and a daily routine (12 hr light/12 hr dark cycle). The animal experiments were done in accordance with international guidelines for laboratory animal use and care and approved by the Institutional Research Ethics Committee of Isfahan University of Medical Sciences (ID: IR.MUI.AEC.1401.019).

For a balanced one-way analysis of variance (ANOVA), a sample size of 42 rats (each group: 6) was required, which provided a statistical power of 85% at α=0.05 with an effect size of 0.3. After 1 week of acclimatization, animals were randomly divided into 7 groups with 6 rats each: the normal saline (NS) group (receiving s.c. injection of NS solution and oral gavage of the drug vehicle as the normal control group), DEX 10 group (receiving DEX 10 mg/kg as the hyperlipidemic control group), the

reference group which received DEX and ATOR 40 mg/kg orally (DEX+ATOR 40), treatment groups which received DEX and free EUP 50 and 100 mg/kg (DEX+EUP 50, DEX+EUP 100), or EUP-NPs 50 and 100 mg/kg orally (DEX+EUP-NPs 50, DEX+EUP-NPs 100) (Xu et al. 2018; Lee et al. 2020). For oral administration in rats, all drugs were dissolved in water using carboxymethyl cellulose 1% and tween 80 as a vehicle, and administered via an intragastric tube. In all groups, the volume of injection was 1 mL/kg, and the oral gavage volume was 5 mL/kg.

All treatments were performed over a period of 7 days (Kumar et al. 2011). On day 8, the blood samples were collected through the retro-orbital sinus in overnight-fasted animals under anesthesia with intraperitoneal injection of ketamine (70 mg/kg)/xylazine (7 mg/kg). The serum specimens were used for biochemical evaluations. After scarification, liver samples were removed and examined for histological alterations.

Biochemical/atherogenic indices analysis

The biochemical markers of lipid profile, including total cholesterol, triglycerides, LDL, and high-density lipoprotein (HDL) cholesterol, and biomarkers of liver function, including aspartate aminotransferase (AST) and alanine aminotransferase (ALT) were assessed by colorimetric assay kits according to the manufacturer's procedure. Moreover, the serum atherogenic indices, which strongly predict the risk of atherosclerosis and coronary heart disease, were defined as cardiac risk ratio (CRR) by dividing total cholesterol by triglycerides, atherogenic coefficient (AC) by dividing the cholesterol difference from HDL by HDL, and atherogenic index of plasma (AIP) as the logarithm of the ratio of triglycerides to HDL.

Lipid peroxidation assay

For evaluation of lipid peroxidation, the serum content of MDA was determined based on the reaction with thiobarbituric acid in an acidic environment using a colorimetric kit. The absorbance of the final complex was recorded at 532 nm. The standard curve was created using a series of MDA tetrabutyl ammonium dilutions (Safaeian et al. 2018).

Histopathological analysis

The liver samples were fixed in 10% neutral-buffered formalin solution. After sequential steps of processing, tissue specimens were embedded in paraffin blocks and sectioned at 5 μm thickness. Finally, the slides were stained with hematoxylin and eosin (H&E) and observed microscopically for histopathological changes by a blind expert pathologist. The Kleiner score was used to assess liver samples by evaluating the degree of steatosis, inflammation, and parenchymal damage or hepatocyte ballooning. The scores included: Steatosis (0-3; as 0: < 5%, 1: 5%-33%, 2: 34%-66%, and 3: > 66%), lobular inflammation (0-3; as 0: None, 1: < 2, 2: 2-4, and 3: > 4), and ballooning degeneration (0-2; as 1: Few ballooned cells and 1: Many ballooned cells) (Kleiner et al., 2005).

Statistical analysis

Data is presented as mean ± standard error of mean (SEM) or standard deviation (SD) and was statistically examined by ANOVA followed by Tukey post-hoc test on SPSS 22.0. The p-values <0.05 were considered significant.

Results

Characterization of EUP-NPs

The entrapment efficiency was calculated as 83.60%. The physicochemical characteristics of EUP-NPs, including particle size, zeta potential, PDI, saturated solubility, and drug entrapment efficiency, are shown in Table 1. The saturated solubility of EUP-NPs in water (465.02 ± 3.29 μg/mL) was significantly much higher

than that of free EUP (45.93 ± 2.53 µg/mL) ($p<0.001$).

The drug release profile of EUP-NPs and free EUP is shown in Figure 2. During the first 30 min, the percentage of released drug in both samples was similar; however, the amount of release was gradually changed over time so that after 120 min, the percentage of released drug in EUP-NPs was 94.10 ± 2.36% and in free EUP was 69.03 ± 1.25%.

FTIR spectrum of EUP-NPs

Figure 3 illustrates the FTIR spectra of free EUP and EUP-NPs. In the FTIR spectra of free EUP (Figure 3A), the absorption band at 3279.36 cm^{-1} is attributed to the –OH. The peak at 2873.42 cm^{-1} contributes to the CH2, and the peak at 1641.37 cm^{-1} is attributed to the C=O stretching vibration of the heterocyclic cycle, and the peak at 1131.00 cm^{-1} is related to the C-O. These peaks are seen in EUP-NPs precisely or with a slight shift due to the hydrogen bonding in the composition of the final complex of EUP and chitosan NPs (Figure 3B).

Table 1. Physicochemical characteristics of eupatilin nanoparticles

Particle size (nm)	Zeta potential (mv)	Polydispersity index	Saturated solubility (µg/mL)	Entrapment efficiency (%)
232.60±3.73	3.82±0.13	0.23±0.03	465.02 ± 3.29	83.60

Values are expressed as mean ± SD.

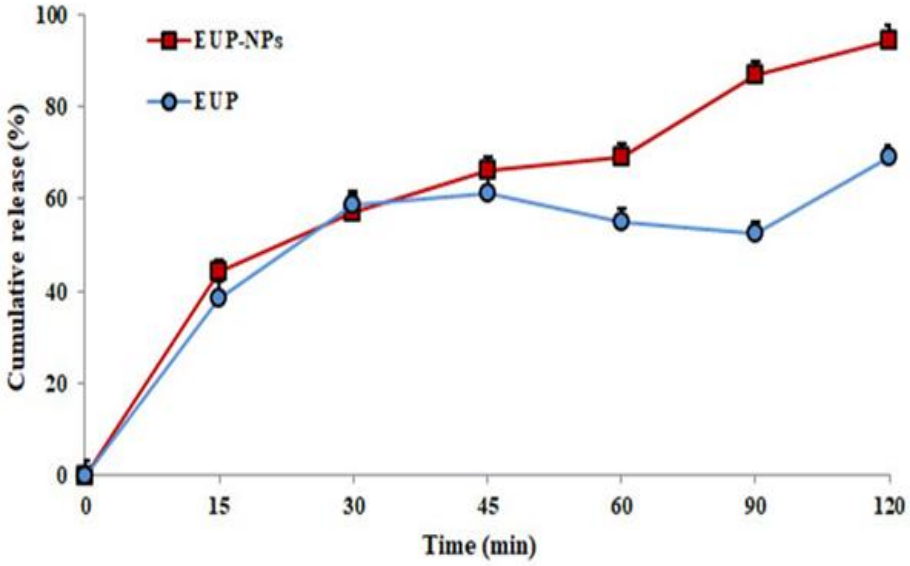

Figure 2. *In vitro* release profile of eupatilin (EUP) from eupatilin nanoparticles (EUP-NPs) and free EUP in PBS medium containing DMSO (0.5%) at 37°C and a pH of 7.4 (n=3).

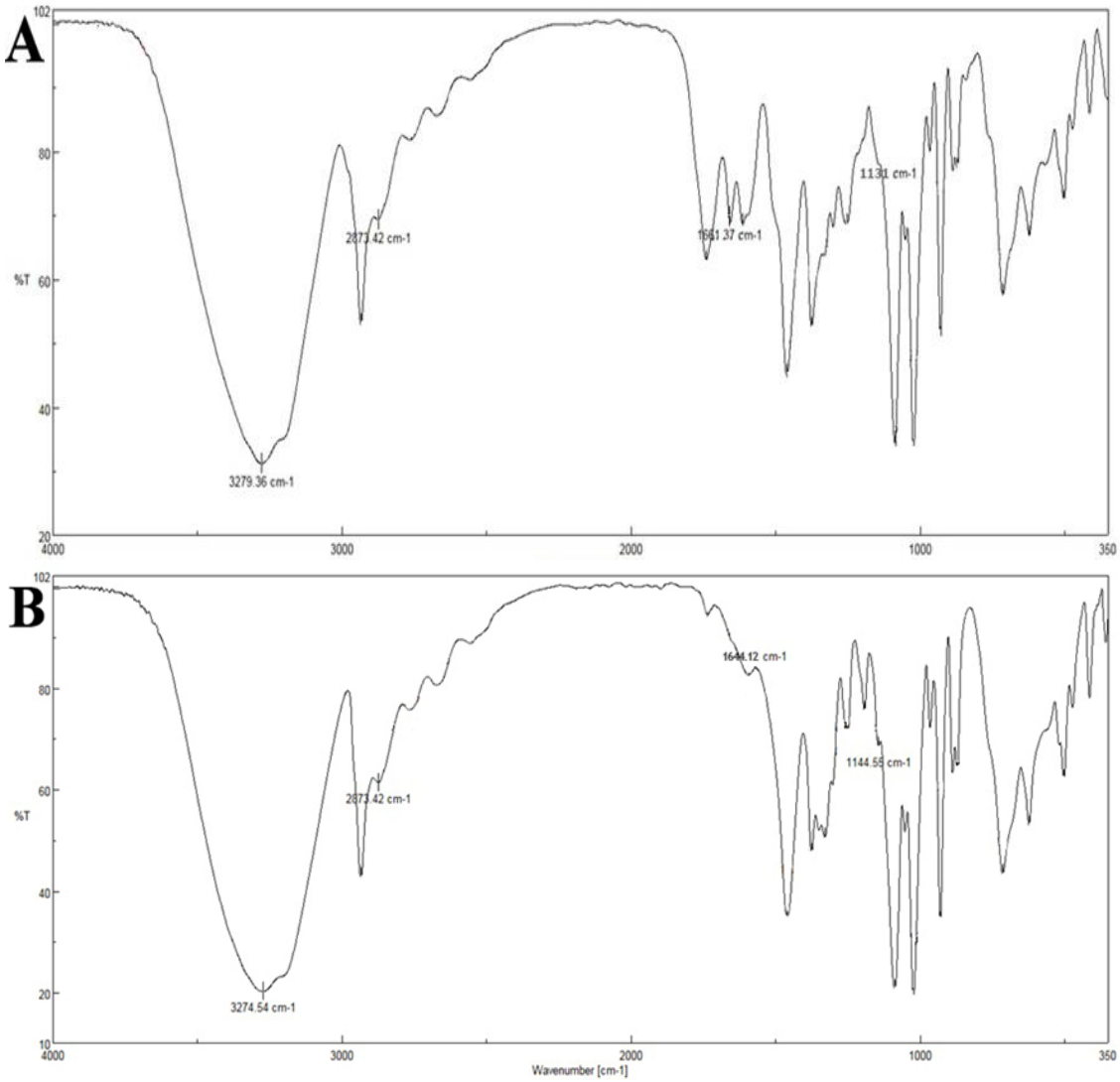

Figure 3. FTIR spectra of free eupatilin (A) and eupatilin nanoparticles (B).

Effect of EUP-NPs on biochemical parameters/atherogenic indices

The effect of EUP-NPs on biochemical parameters of lipid profile and liver injury in DEX-induced hyperlipidemic rats is shown in Figure 4 and 5, respectively. After administration of DEX, hyperlipidemia was induced in rats as demonstrated by significant elevation in serum triglyceride ($p<0.001$), total cholesterol ($p<0.01$), and LDL ($p<0.05$) levels compared to the normal group. No significant change was observed in the HDL level. Moreover, DEX led to the increased atherogenic indices, including CRR ($p<0.01$), AC ($p<0.01$), and AIP ($p<0.001$) (Table 2). The damaging effect of DEX on liver tissue was demonstrated by increased ALT ($p<0.001$) and AST ($p<0.05$) activities. Administration of the reference antihyperlipidemic drug (ATOR) potently reduced the serum concentration of triglycerides (48.54%), total cholesterol (22.02%), and LDL (27.99%), as well as CRR (28.12%), AC (43.08%), AIP (62.74%) and serum activity of AST (24.27%) in comparison with DEX control group without any significant outcome on the ALT activity. The hyperlipidemic rats treated with EUP-NPs showed a remarkable decline in serum lipid parameters at its higher dose. EUP-NPs at the dose of 100 mg/kg decreased triglycerides by 47.02%, total cholesterol by 20.55%, LDL by 28.69%, CRR by 34.72%, AC by 53.19% and AIP by 66.67%. Furthermore, EUP-

NPs lessened the activities of ALT by 22.77% and AST by 27.09% ($p<0.05$) as compared to DEX control group. Treatment of animals with free EUP (100 mg/kg) also reduced triglycerides by 34.81% and AIP by 41.17% ($p<0.05$) compared to DEX group; however, it did not significantly alter the other biochemical markers and atherogenic indices.

Table 2. Effects of free eupatilin and eupatilin nanopaticles on atherogenic indices and liver histopathological alterations in dexamethasone-induced hyperlipidemic rats.

Groups	Atherogenic indices			Liver histopathological alterations		
	CRR	AC	AIP	Steatosis	Inflammation	Ballooning
NS	1.93 ± 0.91	0.93±0.09	0.07±0.03	0	0	0
DEX 10	2.88±0.34$^{\#\#}$	1.88±0.34$^{\#\#}$	0.51±0.04$^{\#\#\#}$	3	2	2
DEX+ATOR 40	2.07±0.09*	1.07±0.09*	0.19±0.51**	1	0	1
DEX+EUP 50	2.93±0.10	1.93±0.10	0.47±0.03	3	2	2
DEX+EUP-NPs 50	2.33±0.07	1.33±0.07	0.34±0.07	2	1	1
DEX+EUP 100	2.44±0.09	1.44±0.24	0.30 ± 0.04*	1	0	1
DEX+EUP-NPs 100	1.88±0.08**	0.88±0.08**	0.17±0.04***	1	0	1

Values are mean ± SEM, n = 6. $^{\#\#}p<0.01$ and $^{\#\#\#}p<0.001$ indicate significant differences compared to NS control group. $^{*}p<0.05$, $^{**}p<0.01$ and $^{***}p<0.001$ indicate significant differences compared to the DEX 10 control. The scores of liver histopathological changes included: Steatosis (0: < 5%, 1: 5%-33%, 2: 34%-66%, and 3: > 66%), lobular inflammation (0: None, 1: < 2, 2: 2-4, and 3: > 4), and ballooning degeneration (1: Few ballooned cells and 2: Many ballooned cells). AC: Atherogenic coefficient; AIP: Atherogenic index of plasma; CRR: Cardiac risk ratio; DEX: Dexamethasone; EUP: Eupatilin; EUP-NPs: Eupatilin-nanopaticles; NS: Normal saline.

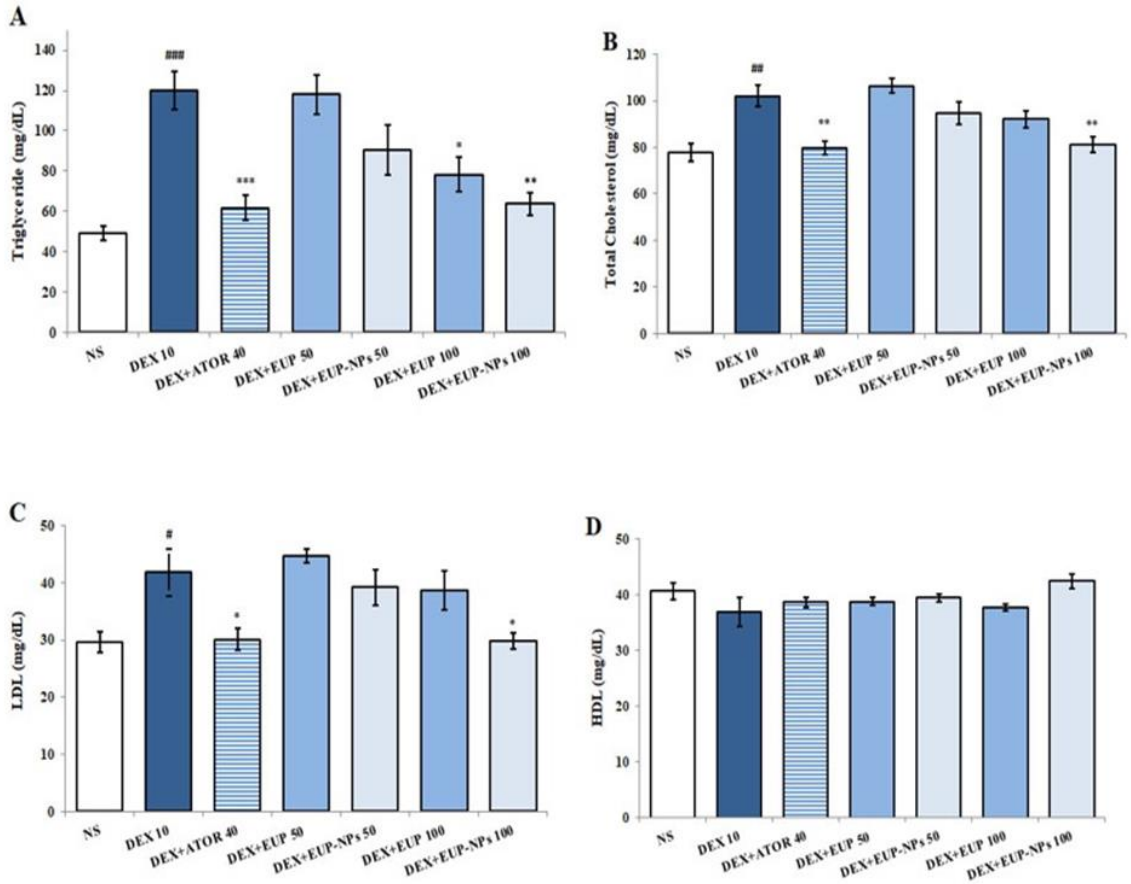

Figure 4. Effects of free eupatilin (EUP), eupatilin nanoparticles (EUP-NPs) (50 and 100 mg/kg) and atorvastatin (ATOR) (40 mg/kg) on serum levels of triglycerides (A), total cholesterol (B), LDL (C), and HDL (D) in dexamethasone (DEX)-induced hyperlipidemia. Values are means ± SEM (n=6). $^{\#}p<0.05$, $^{\#\#}p<0.01$ and $^{\#\#\#}p<0.001$ versus normal saline (NS), and $^{*}p<0.05$, $^{**}p<0.01$ and $^{***}p<0.001$ versus DEX 10.

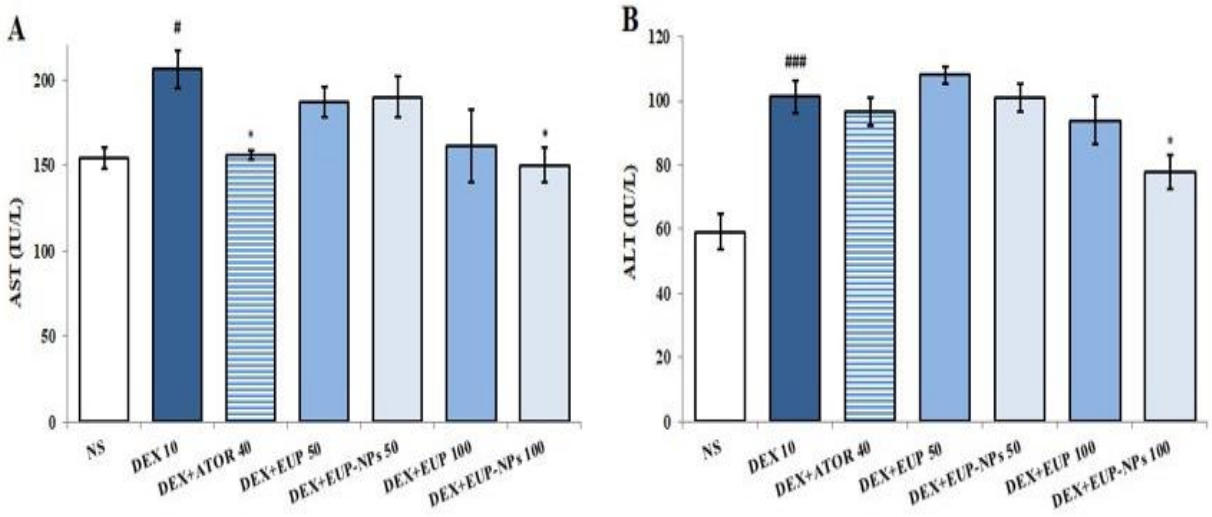

Figure 5. Effects of free patilin (EUP), eupatilin nanoparticles (EUP-NPs) (50 and 100 mg/kg) and atorvastatin (ATOR) (40 mg/kg) on serum activities of AST (A) and ALT (B) in dexamethasone (DEX)-induced hyperlipidemia. Values are means ± SEM (n=6). $^{\#}p<0.05$ and $^{\#\#\#}p<0.001$ versus normal saline (NS), and $^{*}p<0.05$ versus DEX 10.

Effect of EUP-NPs on lipid peroxidation

Evaluation of lipid peroxidation demonstrated that DEX significantly augmented serum MDA concentration ($p<0.05$). Conversely, a notable decline was observed in MDA level after administration of EUP-NPs (50 and 100 mg/kg) ($p<0.05$ and $p<0.01$, respectively) in DEX-induced hyperlipidemic rats (Figure 6).

Effect of EUP-NPs on liver histopathology

Results obtained from liver tissue examination are shown in Figure 7 and summarized in Table 2. No histopathological alterations were observed for the control group (Figure 7A). Animals receiving DEX showed moderate lobular infiltration, many ballooned hepatocytes, and diffused microvesicular steatosis and fatty degeneration of hepatic parenchymal cells (Figure 7B). In rats treated with atorvastatin, there was mild vesicular steatosis and a few ballooned hepatocytes (Figure 7C); groups treated with EUP 50 (Figure 7D) and 100 mg/kg (Figure 7E) showed low inflammation, many to a few ballooned hepatocytes with high to low vesicular steatosis. Rats treated with EUP of 50 (Figure 7F) and 100 mg/kg (Figure 7G) exhibited moderate to low vesicular steatosis with a few ballooned hepatocytes.

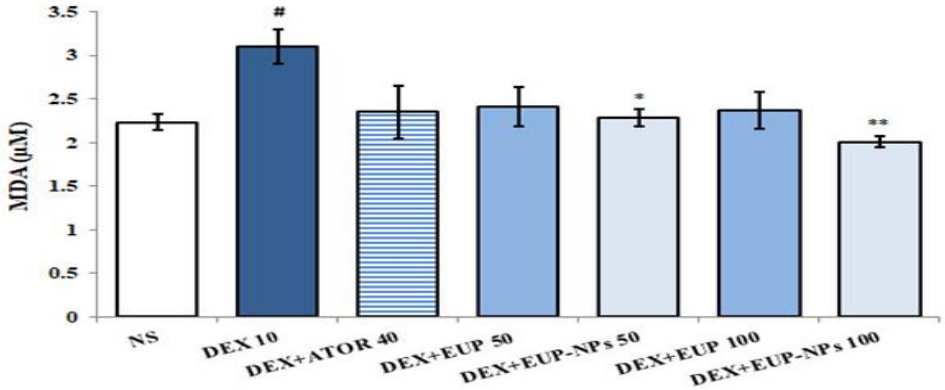

Figure 6. Effects of free eupatilin (EUP), eupatilin nanoparticles (EUP-NPs) (50 and 100 mg/kg) and atorvastatin (ATOR) (40 mg/kg) on serum MDA level in dexamethasone (DEX)-induced hyperlipidemia. Values are means ± SEM (n=6). $^{\#}p<0.05$ versus normal saline (NS), and $^{*}p<0.05$ and $^{**}p<0.01$ versus DEX 10.

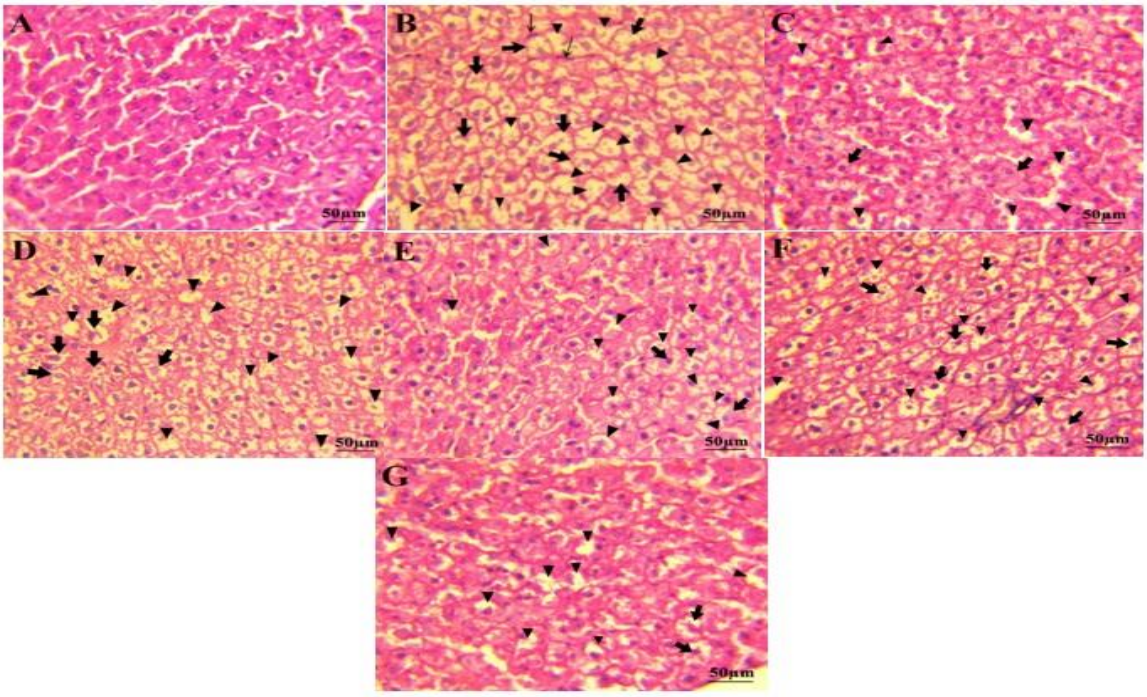

Figure 7. Representative H & E histological sections of the liver tissue of normal control group (A) showing normal hepatocytes appearance; dexamethasone-induced hyperlipidemic group showing infiltration of inflammatory cells, hepatocyte ballooning, and high diffused microvesicular steatosis and fatty degeneration (B); atorvastatin-treated group showing mild vesicular steatosis and ballooning degeneration (C); eupatilin-treated groups with doses of 50 mg/kg (D) and 100 mg/kg (E) showing high to low vesicular steatosis and hepatocyte ballooning; eupatilin nanoparticles-treated groups with doses of 50 mg/kg (F) and 100 mg/kg (G) showing moderate to low vesicular steatosis and a few hepatocyte ballooning. Thin arrows indicate inflammation; Thick arrows indicate hepatocyte ballooning; Triangles indicate steatosis and fatty degeneration. ×400 magnification.

Discussion

This investigation focused on the effect of nano-formulation of EUP in the form of EUP-NPs on its solubility, alongside comparing the impact of EUP-NPs with free EUP on serum lipid profile and MDA level in DEX-induced hyperlipidemic rats.

The N-acetyl derivative of chitin, known as chitosan, is used as an oral delivery carrier. Chitosan NPs have the ability to traverse the small intestinal epithelium through either the paracellular or transcellular pathways (Wang et al. 2011; Divya and Jisha 2018). Some studies reported that chitosan can improve the dissolution of various compounds in water (Soleimanifard et al. 2023; Sharma et al. 2019).

Our results displayed proper particle size for EUP-NPs with a zeta potential value of 3.82 ± 1.25 mV. Since the absolute zeta potential value was under 30 mV, this suggests that the particles are unstable in dispersed conditions (Németh et al. 2022). Therefore, the EUP-NPs were stored in a freeze-dried form. The PDI value of EUP-NPs was determined as 0.23 ± 0.03. The PDI value as a parameter of uniformity and stability of NPs formation, less than 0.5, reflects an almost uniform particle size distribution for EUP-NPs (Xu et al. 2023). The entrapment efficiency of 83.60% was estimated in the current study. This high percentage of entrapment efficiency may be a result of electrostatic interaction between EUP with a negative charge and the positively charged amino groups of chitosan (Fine et al. 2017; Wang et al. 2011).

The saturated solubility of EUP-NPs increased by approximately ten times relative to that of free EUP, indicating the

solubility enhancement of EUP in water by chitosan. Various investigations have shown that chitosan-based NPs can improve the solubility of the hydrophobic agents through several mechanisms, including formation of hydrogen bonds by interaction of hydroxyl and amino groups of chitosan with drug molecules, converting the crystalline form of drugs into an amorphous form, and trapping the hydrophobic drug in the polymer structure, allowing it to better dissolve (Kesharwani et al. 2024). Evaluation of the in vitro drug release exhibited that a rapid release behavior was initially similar for EUP-NPs and EUP; however, after about 45 min, the release of EUP-NPs began to exceed that of the free EUP may be due to the slower dissolution rate of EUP. Furthermore, the full release of EUP-NPs was obtained at 120 min. In many studies, the chitosan-NPs created by the ionic gelation method have shown bi-phasic release with an initial burst release of drug in a specific time, followed by a controlled release manner (Herdiana et al. 2022). Finally, our findings from FTIR tests indicated that the loading of EUP with chitosan NPs did not change the structure of the EUP.

In this animal study, exposure to a high dose of DEX led to the development of hyperlipidemia, that confirmed by the progression of steatosis and fatty liver condition, marked elevation in serum markers of lipid profile and lipid peroxidation, and serum liver enzymes.

Treatment with EUP-NPs at the dose of 100 mg/kg significantly reduced serum lipid parameters, including triglycerides, total cholesterol, LDL, and atherogenic index. Moreover, it decreased serum levels of ALT, AST, and MDA, and improved liver histopathological alteration in DEX-induced hyperlipidemic rats. EUP at 100 mg/kg only led to a decrease in triglycerides and LDL levels, although these effects were less than those of EUP-NPs. Different doses of EUP were selected based on the previous studies confirming their safety and efficacy (Xu et al. 2018; Lee et al. 2020). An oral dose of 100 mg/kg in rats corresponds to approximately 16 mg/kg in humans (or about 1100 mg total for a 70 kg adult) (Saadh et al. 2020). Dietary assessment of global flavonoid intake has shown that Iranians consume high levels of flavonoids, particularly flavanols (1652 mg/day), through their food sources (Escobar-Cévoli et al. 2017). In clinical trials, similar doses of flavonoid supplementation have often been used. As an example, Di Lorenzo et al. evaluated the antioxidant effect of a tablet containing 150 mg quercitrin (a plant flavonol), 150 mg rutin (a flavonoid glycoside), and 200 mg hesperidin (a flavanone glycoside) as a dietary supplement in healthy people with a dosage of 1 to 2 tablets per day for two weeks. When taking two tablets, the dose was equivalent to 1000 mg of flavonoids per day (2024).

Some cardiovascular protective effects have been reported for EUP through attenuating oxidative stress, inflammation, coagulation, atherogenic, and adipogenesis conditions (Lu et al. 2023; Son et al. 2013; Kim et al. 2018).

In 2015, Choi et al. introduced EUP as a selective PPARα agonist using a binding assay based on FRET (Förster resonance energy transfer) detection, and established the stimulation of the transcriptional function of PPARα by EUP through a cell-based transactivation method (2015). In an investigation conducted by Kim et al., oral administration of EUP at the dose of 50 mg/kg effectively decreased total cholesterol by 48.1% and triglycerides by 16.6% in mice with hyperlipidemia induced by Triton WR-1339. In their ex vivo study, EUP showed potent inhibitory action against HMG-CoA reductase, which is a critical enzyme in cholesterol biosynthesis (Kim et al., 2023). In another study, EUP reduced the accumulation of lipid and diminished the expression of PPARγ in adipocyte cells (Kim et al. 2018). Lee et al. also reported the hepatoprotective and antihyperlipidemic effects of EUP in an animal model of alcoholic liver. In their

investigation, EUP at the dose of 100 mg/kg reduced triglycerides by about 33% and total cholesterol by about 20% in rats (Lee et al. 2020).

Compared to the findings of the animal study by Kim et al. (2023), EUP-NPs were more effective in reducing triglycerides (47.02%) than total cholesterol (20.55%) in our study and were more consistent with the results of Lee and co-workers (2020). This could be partly due to the species of animal and the experimental model of hyperlipidemia used in the current study. In DEX-induced dyslipidemia, elevation of fatty acids and lipids in serum occurs due to the augmented lipolysis in adipose tissue and increased synthesis of fatty acids in the liver (Safaeian et al. 2024). The triglyceride-lowering effect of EUP-NPs may be due to inhibition of PPARγ, which regulates fatty acid storage (Kim et al. 2018). Fatty acids are the main building blocks of triglycerides, and EUP-NPs may help reduce triglycerides by decreasing the levels of fatty acids. The potent anti-hypertriglyceridemic activity of EUP-NPs may also be related to the selective stimulatory action on PPARα, and subsequently activation of lipoprotein lipase, and enhancing the catabolism of triglyceride-rich particles (Choi et al. 2015).

In the study of Rosa et al., EUP exhibited defensive activities against oxidative injury in fatty acids and cholesterol in HeLa cells by eliminating lipoperoxyl radicals. EUP also suppressed lipogenesis and altered the phospholipid/cholesterol ratio in these cells (2020).

Moreover, several investigations have presented the hepatoprotective activities of EUP in some animal models, such as alcoholic liver disease and hepatic ischemia-reperfusion injury through antioxidative, antiapoptotic, and anti-inflammatory actions (Lee et al. 2020; Lee et al. 2016; Mine 2006).

Although previous studies have shown the antihyperlipidemic activities of EUP, our results revealed significant effects for EUP-NPs, not EUP, on most of the parameters studied. The reason for this could be due to the model chosen to induce hyperlipidemia. The oral absorption and consequently bioavailability of drugs can indeed be altered in animal models in which DEX is used at high doses and causes toxicity. This occurs through multiple mechanisms; DEX may cause gastrointestinal toxicity through stress-induced effects and mucosal injury. It can induce efflux transporters and metabolizing enzymes, and may also lead to gastroparesis or delayed gastric emptying (Yokota et al. 2007; Reichardt et al. 2014; Bourdin et al. 2023).

The major limitation of this study was the lack of exploration of the mechanisms of antihyperlipidemic effects of EUP-NPs. Besides, high doses of dexamethasone are needed for the induction of hyperlipidemia, which is associated with adverse effects, for example, severe body weight loss and skeletal muscle destruction in rats (Dunford and Riddell 2016).

In summary, EUP-loaded chitosan NPs were developed by an ionotropic gelation procedure for oral delivery in this study. The EUP-NPs were prepared with relatively high drug entrapment, desirable particle size, and PDI values, and acceptable release efficiency,, leading to the enhanced solubility of EUP. EUP-NPs showed improved activities in DEX-induced hyperlipidemia, more effective than free EUP by reducing serum levels of triglycerides, total cholesterol, LDL, atherogenic indices, lipid peroxides, and transaminases, and refining liver steatosis.

Acknowledgment

This work was financially supported by Isfahan University of Medical Sciences (Grant No. 3401365).

Conflicts of interest

The authors declare no competing interests.

Authors' Contributions

Conceptualization, Supervision, and Methodology: Z.Y, L.S, E.G; Data collection: S.G; Data analysis: Z.Y, L.S, E.G; Writing – original draft: S.G; Review & editing: L.S, E.G.

Abbreviations

AC: Atherogenic coefficient, AIP: Atherogenic index of plasma; ALT: Alanine aminotransferase; AST: Aspartate aminotransferase; ATOR: Atorvastatin; CRR: Cardiac risk ratio, DEX: Dexamethasone; DMSO: Dimethyl sulfoxide; EUP: Eupatilin; EUP-NPs: EUP-loaded chitosan nanoparticles; FRET: Förster resonance energy transfer; FTIR: Fourier transform infrared; HDL: High-density lipoprotein; H&E: Hematoxylin and eosin; HMG-CoA: 3-Hydroxy-3-methylglutaryl-coenzyme A; IL: Interleukin; LDL: Low-density lipoproteins; MDA: Malondialdehyde; MPLC: Medium-pressure liquid chromatography; NMR: Nuclear magnetic resonance; NPs: Nanoparticles; NS: Normal saline; PBS: Phosphate buffer saline; PDI: Polydispersity index; PPAR: Peroxisome proliferator-activated receptor; TLC: Thin layer chromatography; TNF: Tumor necrosis factor; TPP: Tripolyphosphate.

References

Bourdin V, Bigot W, Vanjak A, et al. (2023) Drug–drug interactions involving dexamethasone in clinical practice: myth or reality? J Clin Med 12:7120. doi: 10.3390/jcm12227120

Choi Y, Jung Y, Kim SN (2015) Identification of eupatilin from *Artemisia argyi* as a selective PPARα agonist using affinity selection ultrafiltration LC-MS. Molecules 20:13753-13763. doi: 10.3390/molecules200813753

Dunford EC, Riddell MC (2016) The metabolic implications of glucocorticoids in a high-fat diet setting and the counter-effects of exercise. Metabolites 6:44. doi: 10.3390/metabo6040044

Divya K, Jisha MS (2018) Chitosan nanoparticles preparation and applications. Environ Chem Lett 16:101-112. doi: 10.1007/s10311-017-0670-y

Escobar-Cévoli R, Castro-Espín C, Béraud V, Buckland G, Zamora-Ros R, Béraud GB (2017) An overview of global flavonoid intake and its food sources. Flavonoids-from Biosynthesis to Human Health. IntechOpen 23:1-20. doi: 10.5772/67655

Fine D, Wherritt D, Sumner L (2017) Eupatilin; LC-ESI-QTOF; MS2; CE:50 eV; [M-H]-. MassBank Record: MSBNK-BS-BS003602. Plant Biology, The Noble Foundation, Ardmore, OK, US/. https://massbank.eu/MassBank/RecordDisplay?id=MSBNK-BS-BS003602

Geng P, Luo X, Peng X, et al. (2018) Development and validation of UPLC–MS/MS method for determination of eupatilin in rat plasma and its application in a pharmacokinetics study. Acta Chromatogr 30:231-235. doi: 10.1556/1326.2017.00320

Herdiana Y, Wathoni N, Shamsuddin S, Muchtaridi M (2022) Drug release study of the chitosan-based nanoparticles. Heliyon 8:e08674. doi: 10.1016/j.heliyon.2021.e08674

Hu J, Johnston KP, Williams III RO (2004) Nanoparticle engineering processes for enhancing the dissolution rates of poorly water-soluble drugs. Int J Pharm 273:233-245. doi: 10.1081/ddc-120030422

Jang JM, Park KJ, Kim DG, et al. (2003) Pharmacokinetics of a new antigastritic agent, eupatilin, an active component of Stillen, in rats. J Appl Pharmacol 11:163-168.

Jiang N, Doseff AI, Grotewold E (2016) Flavones: from biosynthesis to health benefits. Plants 5:27. doi: 10.3390/plants5020027

Kawasaki T, Kambayashi JI, Ariyoshi H, Sakon M, Suehisa E, Monden M (1997) Hypercholesterolemia as a risk factor for deep-vein thrombosis. Thromb Res 88:67-73. doi: 10.1016/s0049-3848(97)00192-8.

Kesharwani P, Halwai K, Jha SK, et al. (2024) Folate-engineered chitosan nanoparticles: next-generation anticancer nanocarriers. Mol Cancer 23:244. doi: 10.1186/s12943-024-02163-z

Kim JS, Lee SG, Min K, et al. (2018) Eupatilin inhibits adipogenesis through suppression

of PPARγ activity in 3T3-L1 cells. Biomed Pharmacol 103:135–139. doi: 10.1016/j.biopha.2018.03.073

Kim KJ, Kang NE, Oh YS, Jang SE (2023) Eupatilin alleviates hyperlipidemia in mice by inhibiting HMG-CoA reductase. Biochem Res Int 2023:8488648. doi: 10.1155/2023/8488648

Kleiner DE, Brunt EM, Van Natta M, et al. (2005) Design and validation of a histological scoring system for nonalcoholic fatty liver disease. Hepatology 41:1313–1321. doi: 10.1002/hep.20701

Kumar VS, Inamdar MN, Viswanatha GL (2011) Protective effect of lemongrass oil against dexamethasone induced hyperlipidemia in rats: possible role of decreased lecithin cholesterol acetyl transferase activity. Asian Pac J Trop Med 4:658-660. doi: 10.1016/S1995-7645(11)60167-3.

Kunjachan S, Jose S, Lammers T (2010) Understanding the mechanism of ionic gelation for synthesis of chitosan nanoparticles using qualitative techniques. Asian J Pharm 4. doi: 10.22377/ajp.v4i2.220

Lee HM, Jang HJ, Kim SS, et al. (2016) Protective effect of eupatilin pretreatment against hepatic ischemia-reperfusion injury in mice. Transpl Proc 48:1226–1233. doi: 10.1016/j.transproceed.2016.01.024

Lee HY, Nam Y, Choi WS, et al. (2020) The hepato-protective effect of eupatilin on an alcoholic liver disease model of rats. Korean J Physiol Pharmacol 24:385–394. doi: 10.4196/kjpp.2020.24.5.385

Lu Y, Li D, Huang Y, et al. (2023) Pretreatment with Eupatilin attenuates inflammation and coagulation in sepsis by suppressing JAK2/STAT3 signaling pathway. J Inflamm Res 16:1027–1042. doi: 10.2147/JIR.S393850

Min SW, Kim NJ, Baek NI, Kim DH (2009) Inhibitory effect of eupatilin and jaceosidin isolated from *Artemisia princeps* on carrageenan-induced inflammation in mice. J Ethnopharmacol 125:497-500. doi: 10.1016/j.jep.2009.06.001

Mine T (2006) Eupatilin has an antiapoptotic action on hepatocytes, in contrast to apoptotic actions on other cells. J Gastroenterol 41:818–819. doi: 10.1007/s00535-006-1861-7

Nageen B, Sarfraz I, Rasul A, et al. (2020) Eupatilin: a natural pharmacologically active flavone compound with its wide range applications. J Asian Nat Prod Res 22:1-16. doi: 10.1080/10286020.2018.1492565

Nasrullah PR, Sehar B, Safdar M, et al (2023) Effect of Ajwa date pits powder (*Phoenix dactylifera* L.) on body composition, lipid profile and blood pressure in patients with hyperlipidemia: A randomized clinical trial. Avicenna J Phytomed 13:143-152. doi: 10.22038/ajp.2022.21316

Németh Z, Csóka I, Semnani Jazani R, et al. (2022) Quality by design-driven zeta potential optimisation study of liposomes with charge imparting membrane additives. Pharmaceutics 14:1798. doi: 10.3390/pharmaceutics14091798

Poznyak AV, Nikiforov NG, Markin AM, et al. (2021) Overview of OxLDL and its impact on cardiovascular health: focus on atherosclerosis. Front Pharmacol 11:613780. doi: 10.3389/fphar.2020.613780

Qiao HB, Li J, Lv LJ, et al. (2018) Eupatilin inhibits microglia activation and attenuates brain injury in intracerebral hemorrhage. Exp Ther Med 16:4005-4009. doi: 10.3892/etm.2018.6699

Reichardt SD, Weinhage T, Rotte A, et al. (2014) Glucocorticoids induce gastroparesis in mice through depletion of l-arginine. Endocrinology 155:3899-3908. doi: 10.1210/en.2014-1246

Rodriguez-Garcia M, Alcaide P (2021) Vascular inflammation and hyperlipidemia: the neutrophil within. J Am Coll Cardiol Basic Transl Sci 6:524-526. doi: 10.1016/j.jacbts.2021.05.006

Rosa A, Isola R, Pollastro F, et al. (2020) The dietary flavonoid eupatilin attenuates in vitro lipid peroxidation and targets lipid profile in cancer HeLa cells. Food Funct 11:5179-5191. doi: 10.1039/d0fo00777c

Ryu R, Jung UJ, Kim HJ, et al. (2013) Anticoagulant and antiplatelet activities of *Artemisia princeps* Pampanini and its bioactive components. Prev Nutr Food Sci 18:181-187. doi: 10.3746/pnf.2013.18.3.181

Saadh MJ, Haddad M, Dababneh MF, Bayan MF, Al-Jaidi BA (2020) A guide for estimating the maximum safe starting dose and conversion it between animals and

humans. Syst Rev Pharm 11: 98-101. doi: 10.31838/SRP.2020.8.14

Safaeian L, Ghanadian M, Shafiee-Moghadam Z (2018) Antihyperlipidemic effect of different fractions obtained from *Teucrium polium* hydroalcoholic extract in rats. Int J Prev Med 9:30. doi: 10.4103/ijpvm.IJPVM_100_17

Safaeian L, Yazdiniapour Z, Hajibagher S, Bakhtiari Z, Karimian P (2024) The effect of *Dracocephalum subcapitatum* hydroalcoholic extract on dexamethasone-induced hyperlipidemic rats. Res Pharm Sci 19:319-327. doi: 10.4103/RPS.RPS_148_23

Safaeian L, Zolfaghari B, Karimi S, Talebi A, Ghazvini MA (2018) The effects of hydroalcoholic extract of *Allium elburzense* Wendelbo bulb on dexamethasone-induced dyslipidemia, hyperglycemia, and oxidative stress in rats. Res Pharm Sci 13:22-29. doi: 10.4103/1735-5362.220964

Shaito A, Thuan DT, Phu HT, et al. (2020) Herbal medicine for cardiovascular diseases: efficacy, mechanisms, and safety. Front Pharmacol 11:422. doi: 10.3389/fphar.2020.00422

Suganya V, Vetriselvan S, Velmurugan C, Sarath C (2016) Anti-oxidant and anti-hyperlipidemic activity of *Hemidesmus indicus* in rats fed with high-fat diet. Avicenna J Phytomed 6:516-525. doi: 10.22038/ajp.2016.6466

Sharma M, Sharma R, Jain DK, Saraf A (2019) Enhancement of oral bioavailability of poorly water-soluble carvedilol by chitosan nanoparticles: Optimization and pharmacokinetic study. Int J Biol Macromol 135:246-260. doi: 10.1016/j.ijbiomac.2019.05.162

Soleimanifard S, Saeedi S, Yazdiniapour Z (2023) Isolation of potent antileishmanial agents from *Artemisia kermanensis* Podlech using bioguided fractionation. J Parasit Dis 47:297-305. doi: 10.1007/s12639-023-01569-8

Son JE, Lee E, Seo SG, et al. (2013) Eupatilin, a major flavonoid of *Artemisia*, attenuates aortic smooth muscle cell proliferation and migration by inhibiting PI3K, MKK3/6, and MKK4 activities. Planta Med 79:1009–1016. doi: 10.1055/s-0033-1350621

Sun J, Wang Z, Lin C, et al. (2021) Hypolipidemic effects and preliminary mechanism of chrysanthemum flavonoids, its main components luteolin and luteoloside in hyperlipidemia rats. Antioxidants 10:1309. doi: 10.3390/antiox10081309

Showing Compound Eupatilin (FDB000591) (2025), Available on: https://foodb.ca/compounds/FDB000591#references. In: The Metabolomics Innovation Centre (TMIC). Canadian Institutes of Health Research, Canada Foundation for Innovation, Canada, Alberta.

Tomizawa M, Kawanabe Y, Shinozaki F, et al. (2014) Triglyceride is strongly associated with nonalcoholic fatty liver disease among markers of hyperlipidemia and diabetes. Biomed Rep 2:633-636. doi: 10.3892/br.2014.309

Varshosaz J, Ghassami E, Noorbakhsh A, Minaiyan M, Jahanian-Najafabadi A (2019) Trastuzumab-conjugated nanoparticles composed of poly(butylene adipate-co-butylene terephthalate) prepared by electrospraying technique for targeted delivery of docetaxel. IET Nanobiotechnol 13:829-833. doi: 10.1049/iet-nbt.2018.5363

Vekic J, Stromsnes K, Mazzalai S, Zeljkovic A, Rizzo M, Gambini J (2023) Oxidative stress, atherogenic dyslipidemia, and cardiovascular risk. Biomedicines 11:2897. doi: 10.3390/biomedicines11112897

Wang JJ, Zeng ZW, Xiao RZ, et al. (2011) Recent advances of chitosan nanoparticles as drug carriers. Int J Nanomedicine 6:765-774. doi: 10.2147/IJN.S17296

Wang WL, Chen Y, Tam PK (2025) From bench to bedside: Eupatilin activates antioxidant defenses and reduces fibrosis in experimental cholestasis. Eur J Pediatr Surg (Online ahead of print) doi: 10.1055/a-2676-2832

WHO. World Health Organization (2012) The global health observatory. https://www.who.int/data/gho/indicator-metadata-registry/imr-details/3236. Accessed 14 June 2024.

Xu J, Yıldıztekin M, Han D, et al. (2023) Biosynthesis, characterization, and investigation of antimicrobial and cytotoxic activities of silver nanoparticles using *Solanum tuberosum* peel aqueous extract. Heliyon 9:e19061. doi: 10.1016/j.heliyon.2023.e19061

Xu L, Shi G, Xu Y, Lin G, Zhang W, Yang J (2018) Eupatilin attenuates diabetic nephropathy by upregulating matrix metalloproteinase-9 expression in diabetic rat kidney. Trop J Pharm Res 17:1055-1060. doi: 10.4314/tjpr.v17i6.11

Xu Q, Li YC, Du C, Wang LN, Xiao YH (2021) Effects of apigenin on the expression of LOX-1, Bcl-2, and Bax in hyperlipidemia rats. Chem Biodivers 18:e2100049. doi: 10.1002/cbdv.202100049

Yokota A, Taniguchi M, Takahira Y, Tanaka A, Takeuchi K (2007) Dexamethasone damages the rat stomach but not small intestine during inhibition of COX-1. Dig Dis Sci 52:1452-1461. doi: 10.1007/s10620-006-9273-3

Zhong WF, Wang XH, Pan B, Li F, Kuang L, Su ZX (2016) Eupatilin induces human renal cancer cell apoptosis via ROS-mediated MAPK and PI3K/AKT signaling pathways. Oncol Lett 12:2894-2899. doi: 10.3892/ol.2016.4989.